

Supporting Information for:

**Synthesis and Side Chain Engineering of
Phenylnaphthalenediimide(PNDI)-Based *n*-Type Polymers for
Efficient All-Polymer Solar Cells**

Han-Hee Cho[†], *Taesu Kim*[†], *Kimyung Kim*[§], *Changyeon Lee*[†], *Felix Sunjoo Kim*^{*,§}, and
Bumjoon J. Kim^{*,†}

[†]Department of Chemical and Biomolecular Engineering, Korea Advanced Institute of Science and Technology (KAIST), Daejeon 306-701, Republic of Korea

[§]School of Chemical Engineering and Materials Science, Chung-Ang University, Seoul 06974, Republic of Korea

*Electronic mail: bumjoonkim@kaist.ac.kr, fskim@cau.ac.kr

Table of Contents

Supplementary Figures S1-13

- **Figure S1:** ^1H -NMR spectra of **1a–1c** in CDCl_3 .
- **Figure S2:** ^1H -NMR spectra of **3a–3c** in CDCl_3 .
- **Figure S3:** ^{13}C -NMR spectra of **3a–3c** in CDCl_3 .
- **Figure S4:** ^1H -NMR spectra of (a) PPNDI-EH, (b) PPNDI-BO, and (c) PPNDI-HD in CDCl_3 .
- **Figure S5:** Thermogravimetric analysis curves of newly synthesized *n*-type polymers.
- **Figure S6:** Second cycle heating and cooling DSC curves of PPNDI-EH, PPNDI-BO, and PPNDI-HD
- **Figure S7:** (a) Torsional angles θ_1 ; between the thiophene ring and the NDI core, θ_2 and θ_3 ; between the alkoxyphenyl side chains and the NDI core. (b) Equilibrium geometry and simulated electron density distribution of HOMO and LUMO of the simplified oligomer by DFT with the B3LYP/6-31G* basis set.
- **Figure S8:** Cyclic voltammograms of PPNDI-EH, PPNDI-BO, PPNDI-HD pristine films, and ferrocene (inset).
- **Figure S9.** 2D-GIXS images of (a) pristine and (b) thermally annealed thin films of PPNDI-EH, PPNDI-BO, and PPNDI-HD.
- **Figure S10:** Normalized UV-Vis spectra of the pristine and thermally annealed (300 °C, 1 h) thin films of PPNDI-EH, PPNDI-BO, and PPNDI-HD.
- **Figure S11:** (a-c) Transfer and (d-f) output characteristics for PNDI-based polymers, PPNDI-EH (a,d), PPNDI-BO (b,e), and PPNDI-HD (c,f) in bottom-gate/top-contact OFETs.
- **Figure S12:** (a) UV-Vis absorption spectra and (b) dependence of the J_{SC} on the light intensities of optimized PTB7-Th:PPNDI-EH, PTB7-Th:PPNDI-BO, and PTB7-Th:PPNDI-HD blend films.
- **Figure S13:** (a) 2D-GIXS images and (b) in-plane linecuts (left) and out-of-plane linecuts (right) of PTB7-Th:PPNDI-EH, PTB7-Th:PPNDI-BO, and PTB7-Th:PPNDI-HD blend films.

Supplementary Table S1

- **Table S1:** GIXS parameters of PPNDI-EH, PPNDI-BO, and PPNDI-HD in thin films after thermal annealing.

Supplementary Figures

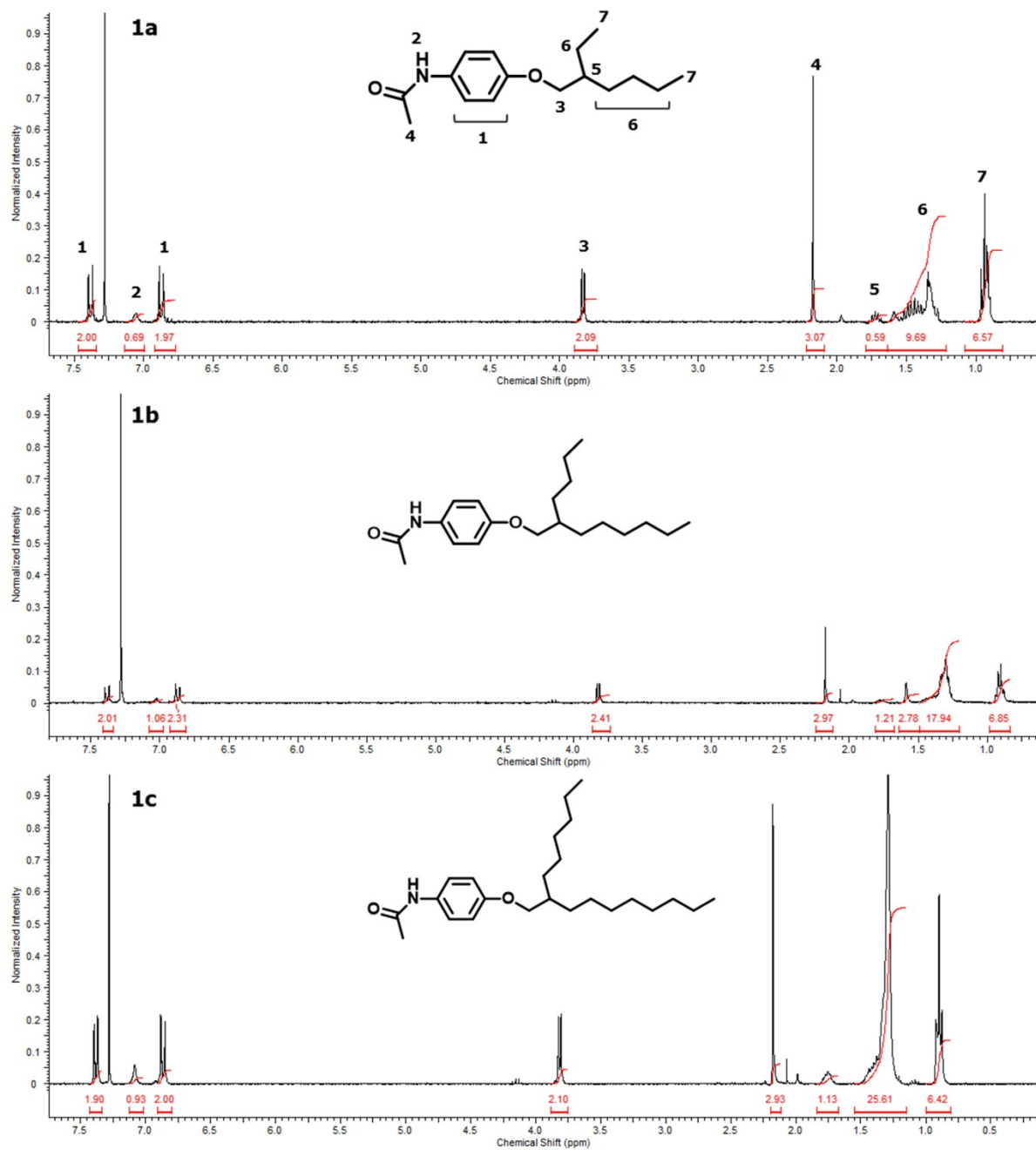


Figure S1. ¹H-NMR spectra of 1a–1c in CDCl₃.

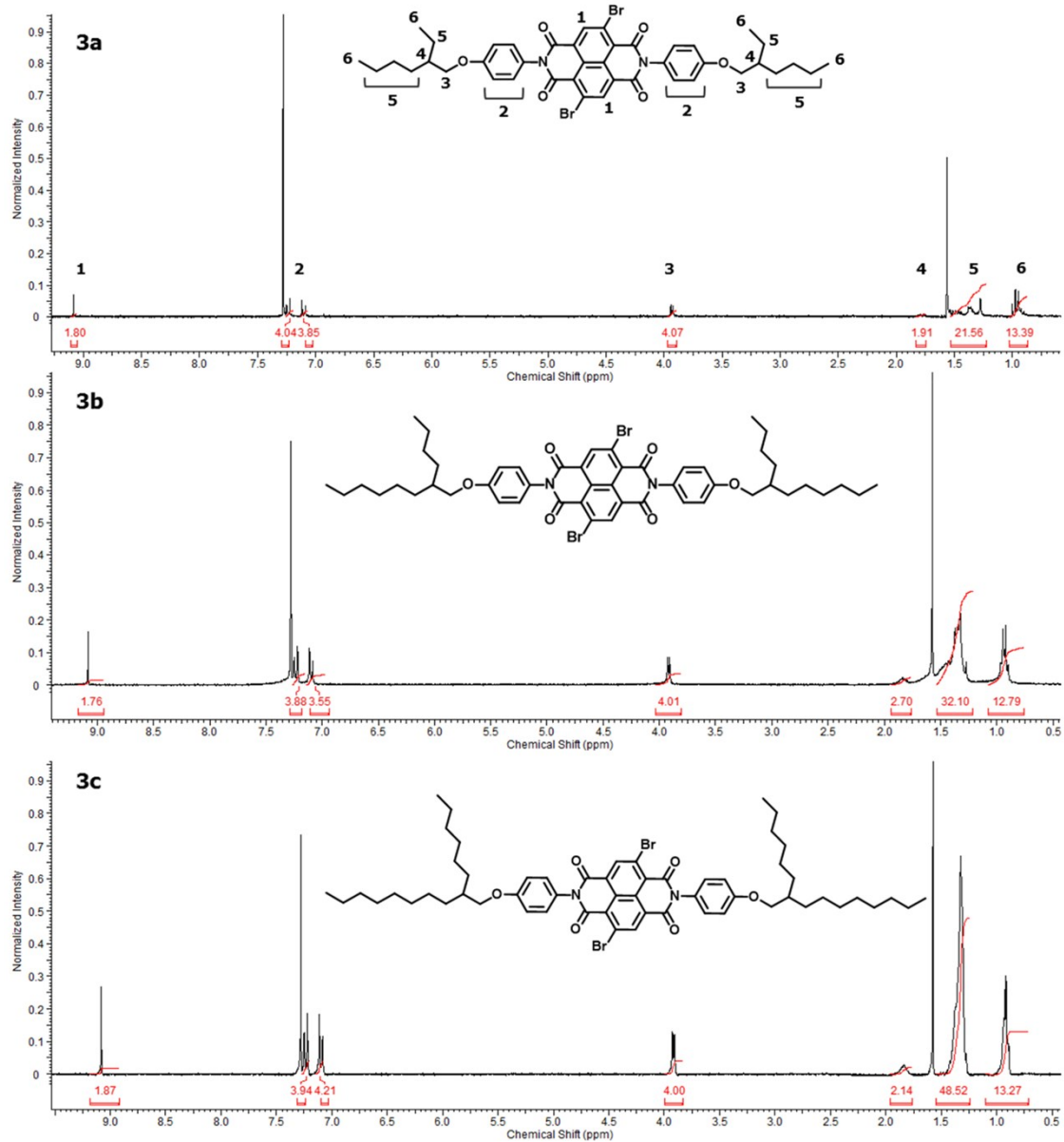


Figure S2. $^1\text{H-NMR}$ spectra of **3a–3c** in CDCl_3 .

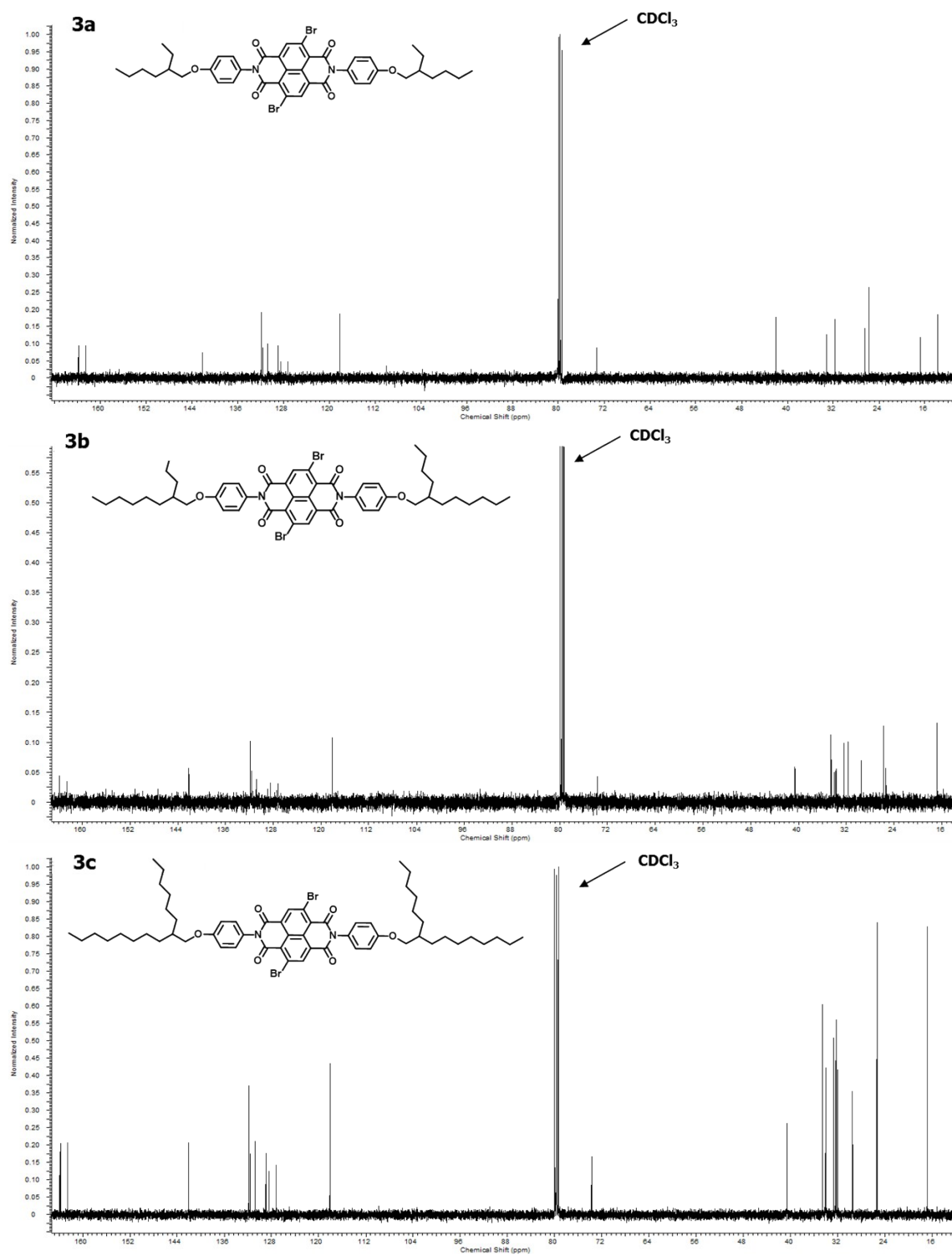
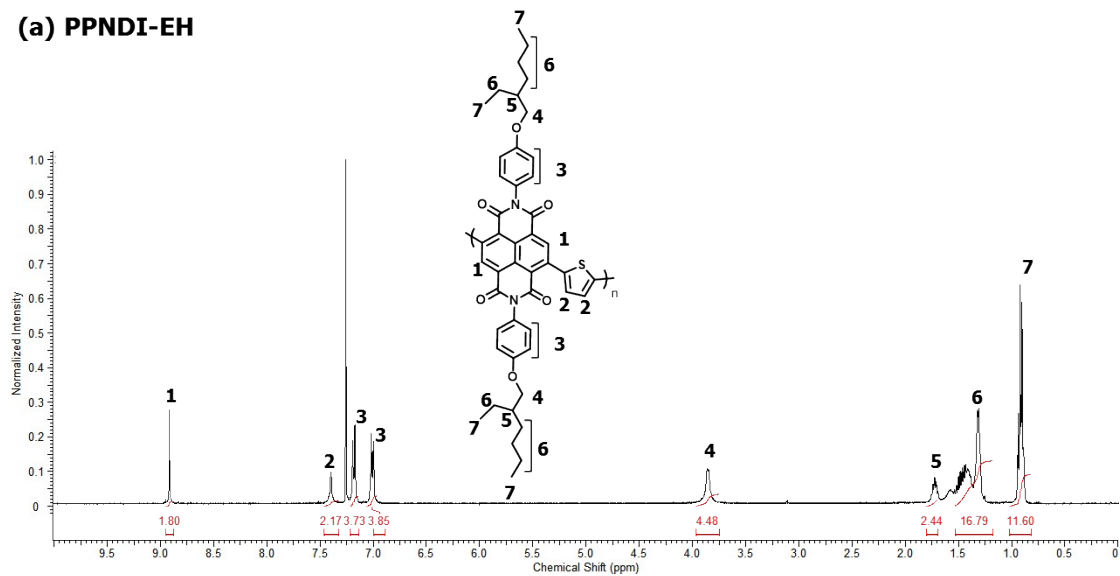
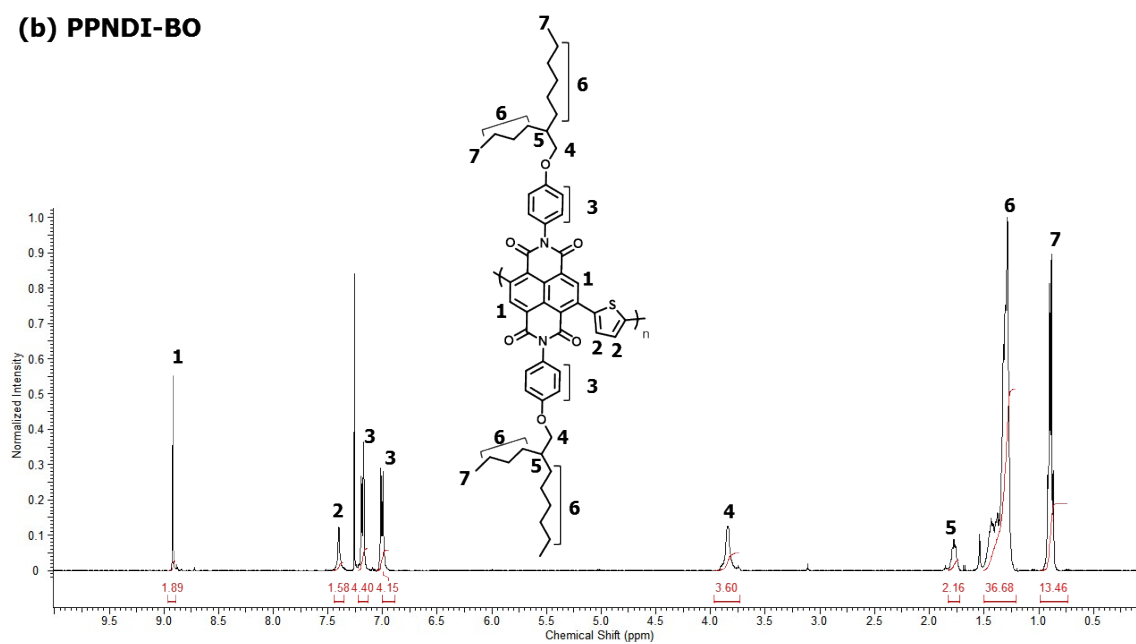


Figure S3. ^{13}C -NMR spectra of **3a–3c** in CDCl_3 .

(a) PPNDI-EH



(b) PPNDI-BO



(c) PPNDI-HD

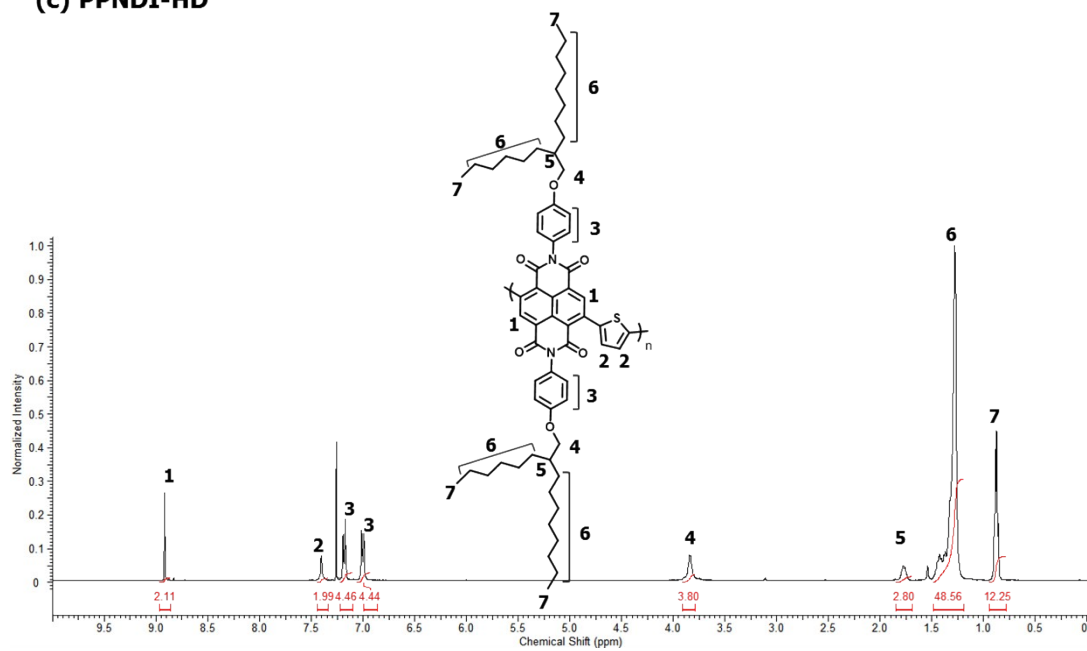


Figure S4. ¹H-NMR spectra of (a) PPNDI-EH, (b) PPNDI-BO, and (c) PPNDI-HD in CDCl₃.

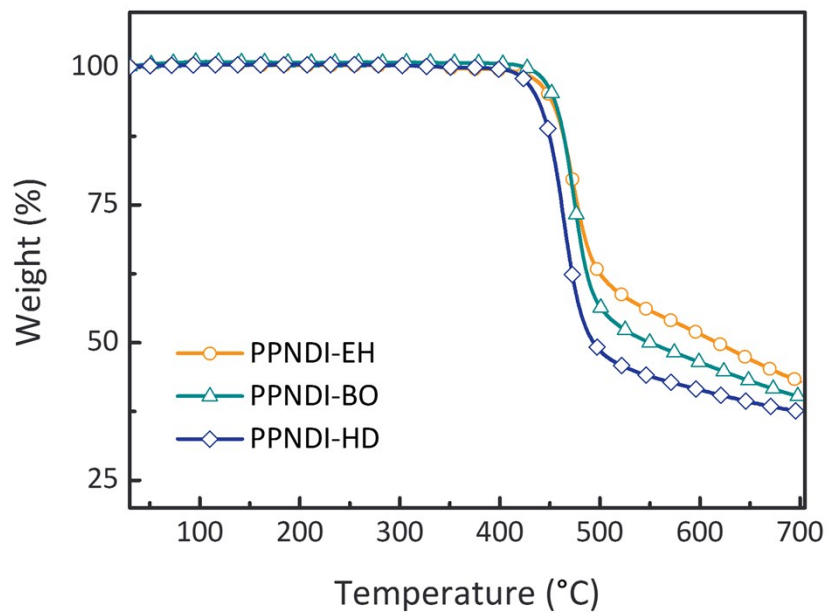


Figure S5. Thermogravimetric analysis curves of newly synthesized *n*-type polymers.

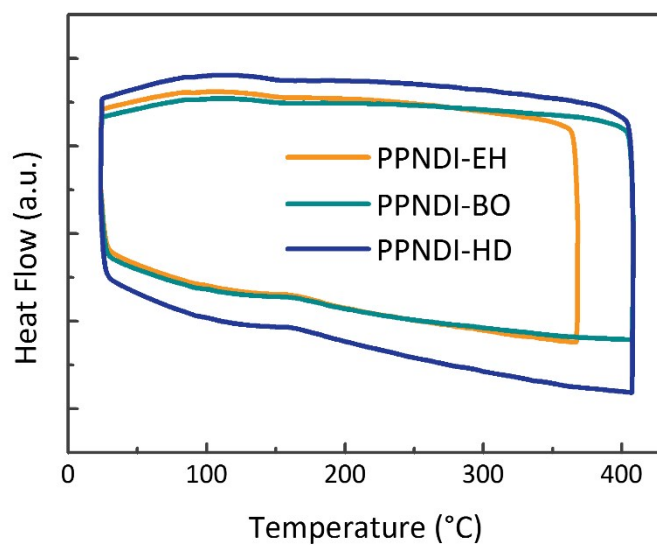


Figure S6. Second cycle heating and cooling DSC curves of PPNDI-EH, PPNDI-BO, and PPNDI-HD

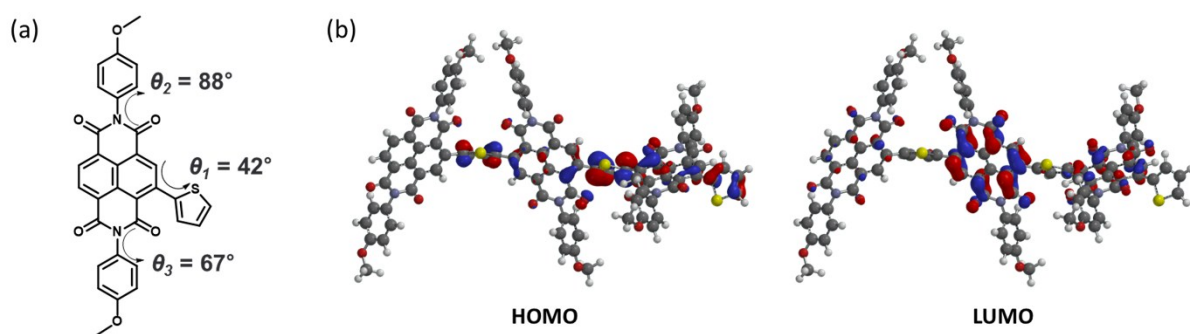


Figure S7. (a) Torsional angles θ_1 ; between the thiophene ring and the NDI core, θ_2 and θ_3 ; between the alkoxyphenyl side chains and the NDI core. (b) Equilibrium geometry and simulated electron density distribution of HOMO and LUMO of the simplified oligomer obtained from DFT calculation with the B3LYP/6-31G* basis set.

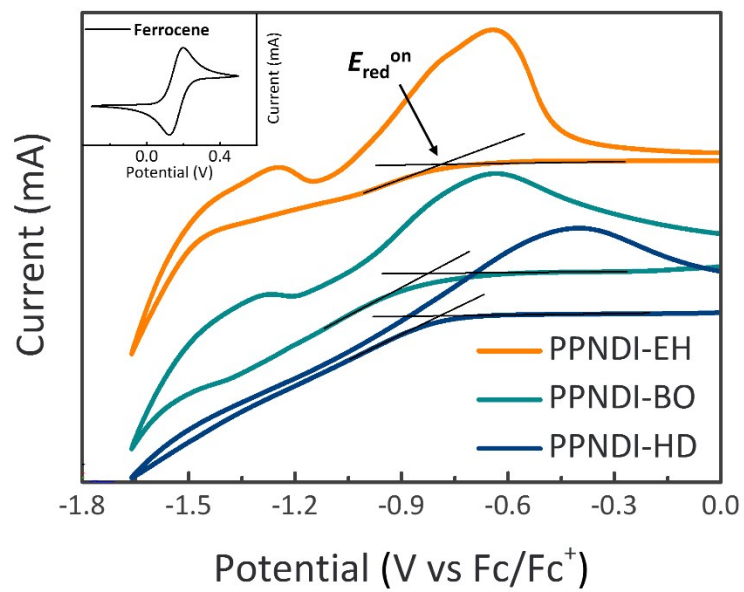


Figure S8. Cyclic voltammograms of PPNDI-EH, PPNDI-BO, PPNDI-HD pristine films, and ferrocene (inset).

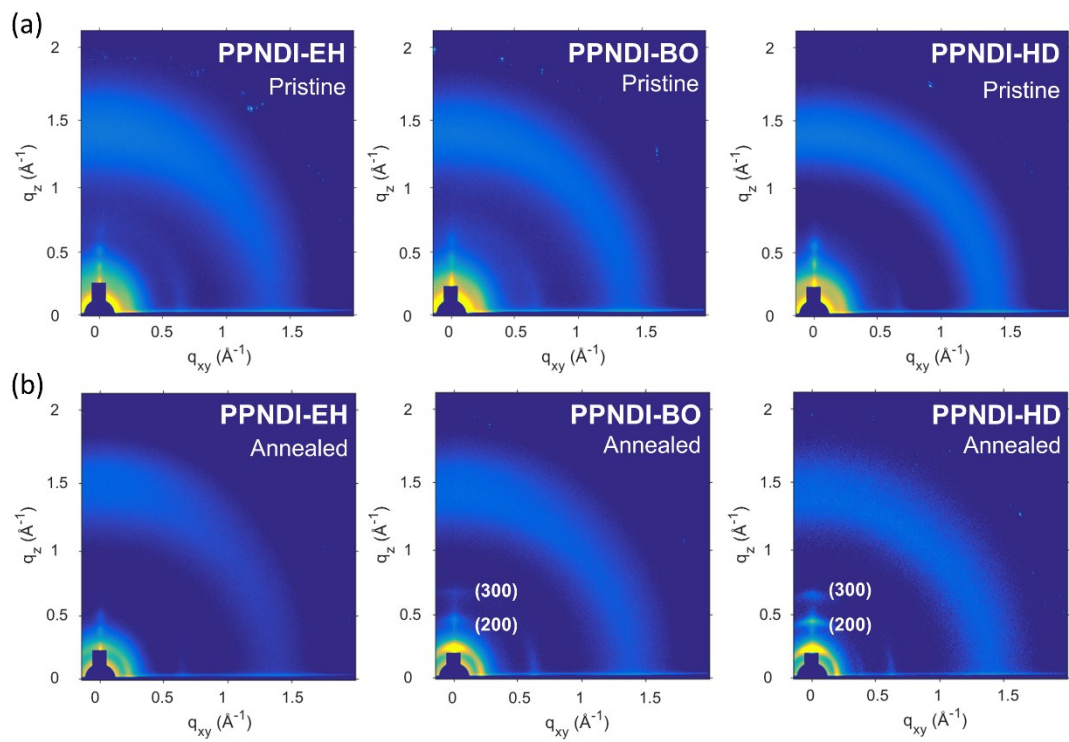


Figure S9. 2D-GIXS images of (a) pristine and (b) thermally annealed thin films of PPNDI-EH, PPNDI-BO, and PPNDI-HD.

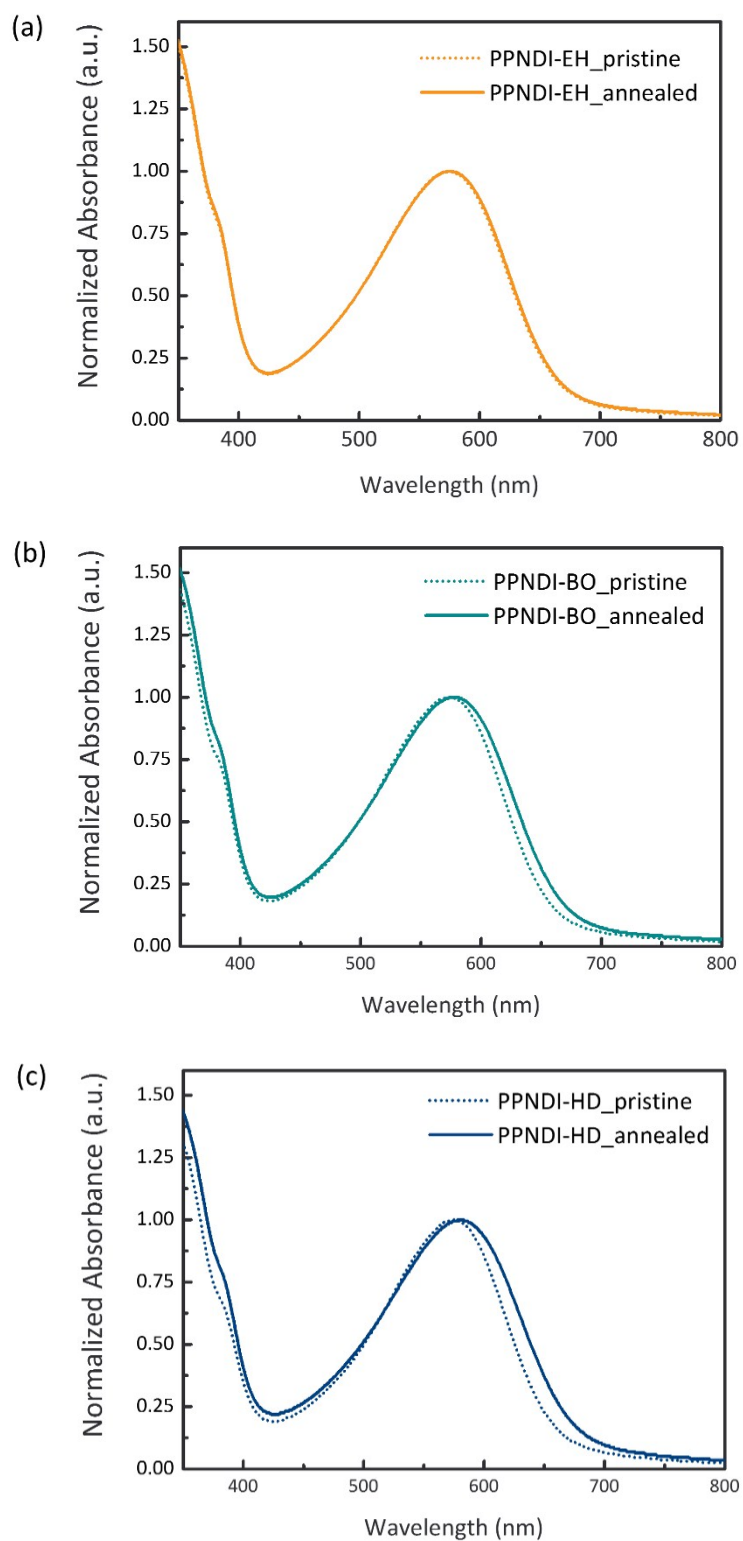


Figure S10. Normalized UV-Vis spectra of the pristine and thermally-annealed (300 °C, 1 h) thin films of PPNDI-EH, PPNDI-BO, and PPNDI-HD.

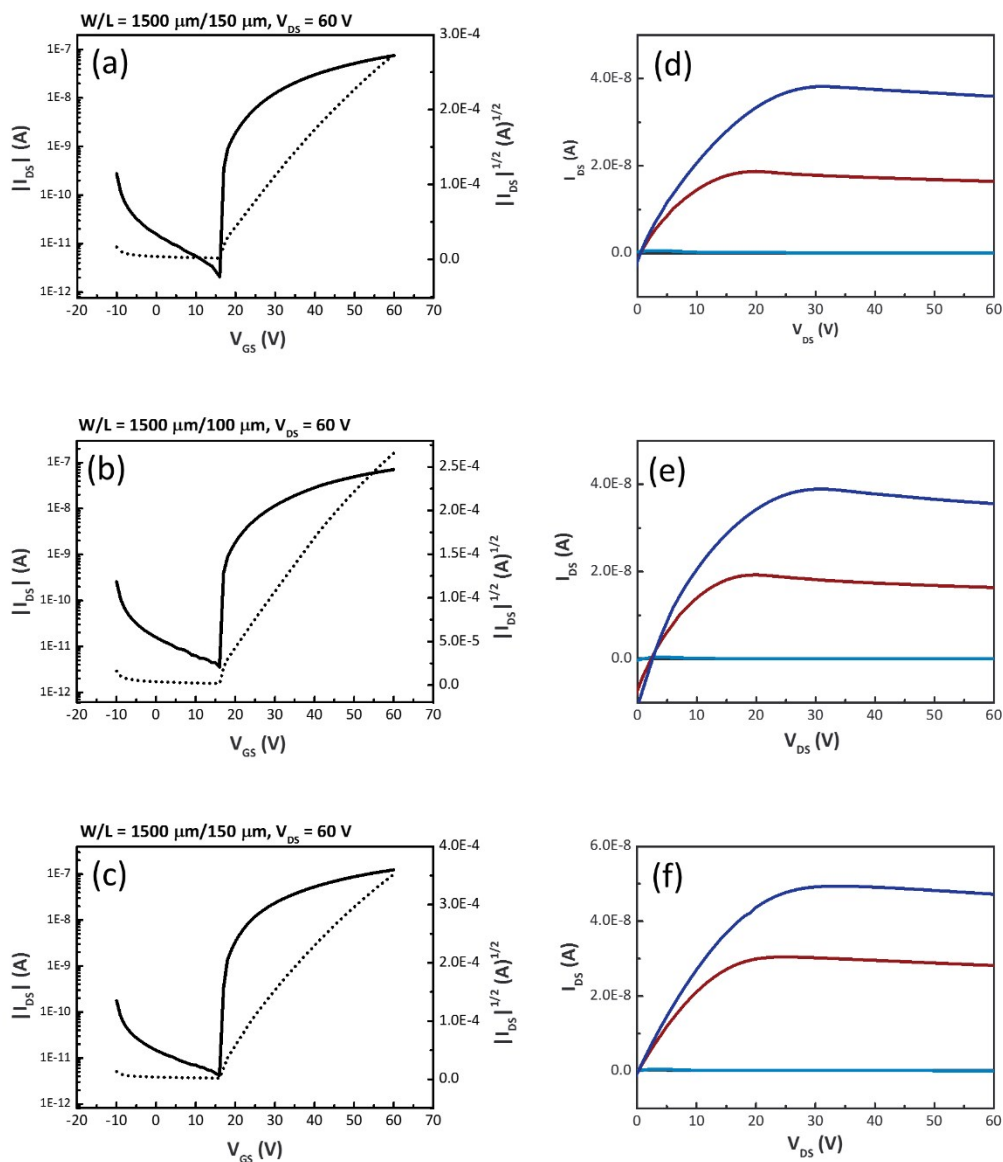


Figure S11. (a-c) Transfer and (d-f) output characteristics for PNDI-based polymers, PPNDI-EH (a,d), PPNDI-BO (b,e), and PPNDI-HD (c,f) in bottom-gate/top-contact OFETs.

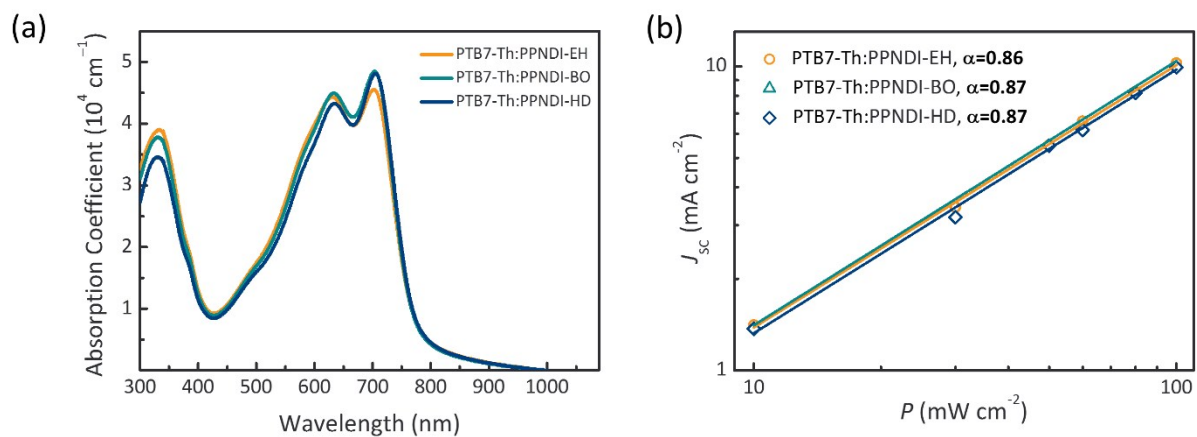


Figure S12. (a) UV-Vis absorption spectra and (b) dependence of the J_{sc} on the light intensities of optimized PTB7-Th:PPNDI-EH, PTB7-Th:PPNDI-BO, and PTB7-Th:PPNDI-HD blend films.

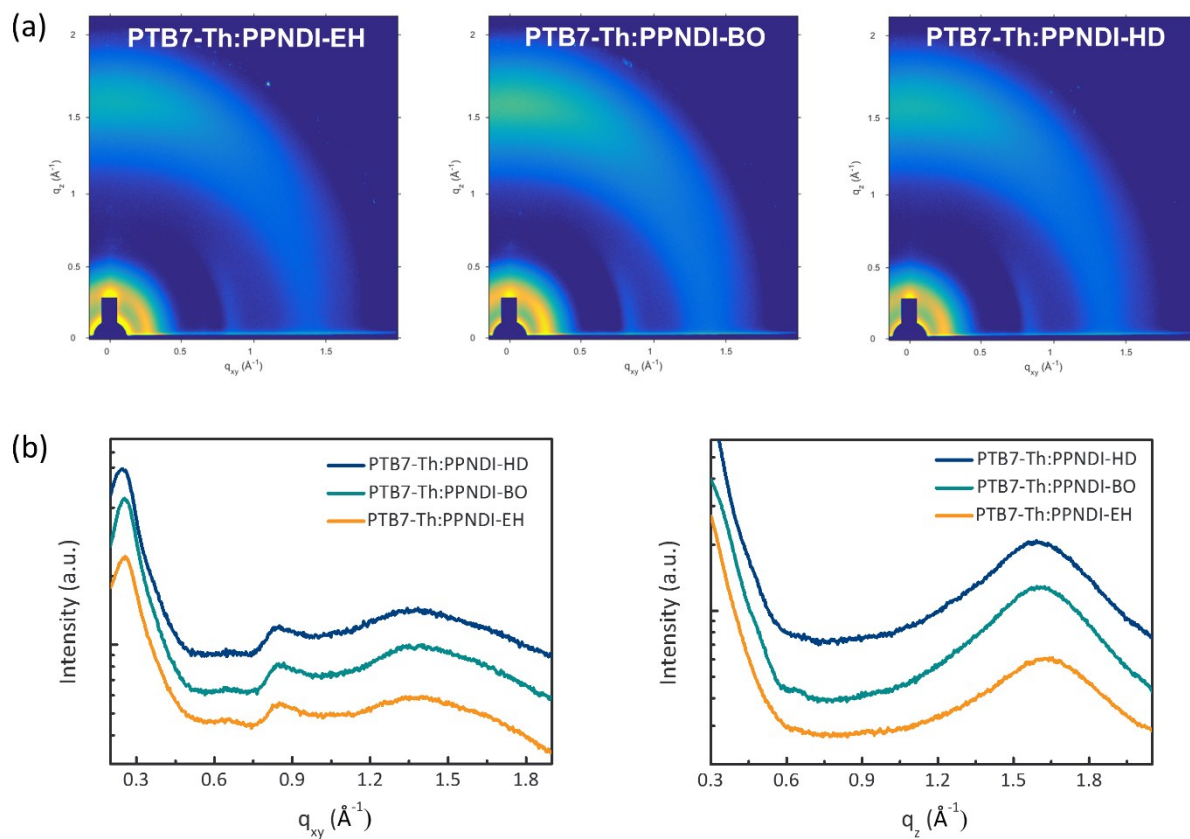


Figure S13. (a) 2D-GIXS images and (b) in-plane linecuts (left) and out-of-plane linecuts (right) of PTB7-Th:PPNDI-EH, PTB7-Th:PPNDI-BO, and PTB7-Th:PPNDI-HD blend films.

Supplementary Table

Table S1. GIXS parameters of PPNDI-EH, PPNDI-BO, and PPNDI-HD in thin films after thermal annealing.

Polymer	In-plane direction	
	$d_{(100)}$ (Å)	$d_{(001)}$ (Å)
PPNDI-EH	27.71	9.55
PPNDI-BO	29.12	9.82
PPNDI-HD	31.52	10.02